Boson peak in overdoped manganites $La_{1-x}Ca_xMnO_3$

B. Gorshunov,[1,2,3] E. Zhukova,[1,2,3] V. I. Torgashev,[4] L. S. Kadyrov,[2,3] E. A. Motovilova,[1,2,3] F. Fischgrabe,[5] V. Moshnyaga,[5] T. Zhang,[6] R. Kremer,[7] U. Pracht,[1] S. Zapf,[1] and M. Dressel[1]

[1]*1. Physikalisches Institut, Universität Stuttgart, Pfaffenwaldring 57, 70550 Stuttgart, Germany*

[2]*A.M. Prokhorov General Physics Institute, Russian Academy of Sciences, 119991 Moscow, Russia*

[3]*Moscow Institute of Physics and Technology (State University), 141700, Dolgoprudny, Moscow Region, Russia*

[4]*Faculty of Physics, Southern Federal University, 344090 Rostov-on-Don, Russia*

[5]*I. Physikalisches Institut, Georg-August-Universität Göttingen, 37077 Göttingen, Germany*

[6]*Key Laboratory of Materials Physics, Institute of Solid State Physics, Chinese Academy of Sciences, Hefei 230031, People's Republic of China*

[7]*Max-Planck-Institut für Festkörperforschung, 70569 Stuttgart, Germany*

(Received 8 March 2013; published 24 June 2013)

In the charge-ordered phase of strongly doped manganites $La_{1-x}Ca_xMnO_3$ ($x \geqslant 0.5$) absorption lines appear in the terahertz spectral range for commensurate x values right below the charge-ordering temperature. They are connected to acoustic phonons that become optically active by folding of the Brillouin zone. At lower temperatures a strongly asymmetric extra absorption band develops at frequencies corresponding to the position of the lowest-energy van Hove singularity in the reduced Brillouin zone. The band is assigned to the boson peak, i.e., to the excess of lattice vibrational states over the standard Debye contribution. The folded phonons and the boson peak do not show up for incommensurate calcium contents when no distinct Brillouin zone folding exists.

DOI: 10.1103/PhysRevB.87.245124 PACS number(s): 63.50.−x, 71.45.Lr, 73.20.Mf, 75.47.Lx

I. INTRODUCTION

Manganites of the family $R_{1-x}A_xMnO_3$ (R is a rare earth and A an alkaline element) provide a unique laboratory to study the physical properties of solids with several competing (or cooperating) order parameters. It is of general importance to understand the transitions to the various single- or multiphase ground states because eventually it may provide ideas for solving fundamental problems in the physics of electronically correlated systems. The task, however, is severely complicated by the diversity of interactions of comparable strength in the charge, magnetic, lattice, or orbital sectors—each trying to stabilize the system according to the corresponding order patterns. For instance, even the well-known colossal negative magnetoresistance effect in hole doped manganites is not understood in all details at this point.[1,2]

Electronically doped (and in particular overdoped) manganites are significantly less studied because they do not exhibit the colossal magnetoresistance effect; instead they demonstrate a dielectric charge-ordered (CO) ground state that can coexist with antiferromagnetic order.[3,4] The origin of the corresponding phase transition has attracted increasing attention in recent years. One of the most popular approaches is based on the charge-density wave (CDW) scenario[5] because the systems seem to possess the necessary ingredients like the Fermi surface nesting and lattice superstructure.[6,7] Low-energy excitations in the THz frequency range are frequently taken as evidence in favor of this mechanism as they are ascribed to the CDW-condensate phase or amplitude modes.[8–12] There is, however, some dispute about this Peierls-Fröhlich scenario.[13,14] In particular, the THz resonances can be consistently interpreted as acoustical lattice vibrations that acquire optical activity when the Brillouin zone is folded due to the superstructure in the CO state.[15–18] This superstructure and corresponding folded phonons are inherent fingerprints of the ordering in manganites. Hence the aim of the present work is to analyze the mechanisms of the corresponding phase transitions by exhaustive exploration of the folded phonons in $La_{1-x}Ca_xMnO_3$ dependent on the calcium content in the broad interval $0.5 \leqslant x \leqslant 1$. An important motivation was also to clarify the role of disorder in the physics of overdoped $La_{1-x}Ca_xMnO_3$ manganites that are available mainly as polycrystals. It is well known that disorder can drastically change the low-energy phonon density of states (DOS) of a solid and can even lead to the appearance of a rather sharp absorption resonance—the so-called boson peak.[19,20] Similar effects are expected in $La_{1-x}Ca_xMnO_3$ for *incommensurate* calcium contents x that lead to a certain degree of disorder in the lattice ion positions. To which extent the disorder-driven renormalization of the phonon DOS is responsible for the low-energy physics of manganites, and in particular for the soft excitations reported in the literature,[8–12,21–24] remains unclear.

II. EXPERIMENTAL DETAILS

Polycrystalline samples $La_{1-x}Ca_xMnO_3$ (LCMO) with $x(\mathrm{Ca}) = 0.5; 0.6; 2/3 \approx 0.67; 0.7; 0.75; 0.85; 0.9; 0.95; 0.98$, and $x = 1$ were prepared by the solid-state reaction method. Stoichiometric amounts of La_2O_3, $CaCO_3$, and MnO were mixed and ground together. The powders were calcined at 1100 °C in air for 12 h, reground, and reacted at 1200 °C for another 12 h. These last steps were repeated three times followed by regrinding and reacting the powders at 1250 °C for 12 h. The resultant materials were pressed into pellets of 2 mm thickness and subsequently sintered again at 1250 °C for 30 h in air. The specimens were slowly cooled to room temperature at a rate of 1 °C/min. All pellets were prepared under identical conditions. The Ca doping was additionally controlled by x-ray diffraction measurements. In addition, epitaxial films were deposited on MgO substrates in a way described in Ref. 25. The films show a strain-free state as indicated by close proximity

of c-axis lattice parameters of films and bulk samples. The CO transition temperatures coincide for films and polycrystalline samples of the same composition.

For optical measurements two kinds of spectrometers were employed: In the range of THz frequencies (3 up to 40 cm^{-1}) we utilized a Mach-Zehnder interferometer based on backward-wave oscillators as coherent radiation sources.[26,27] The permittivity $\epsilon'(\nu)$ and the conductivity $\sigma(\nu)$ spectra were directly determined from the complex transmission coefficient measured through specimens of thickness d between 30 μm and 1 mm. In addition a Fourier-transform spectrometer was utilized to measure the far-infrared reflection coefficient of the same samples, up to $\nu = \omega/(2\pi c) = 700$ cm^{-1}. Kramers-Kronig and dispersion analysis of the reflectivity data in combination with the directly measured THz optical constants allowed us to obtain $\epsilon'(\nu)$ and $\sigma(\nu)$ in the range of approximately 3 to 700 cm^{-1} and at temperatures from 5 to 300 K. The main attention of the present report is focused on excitations detected at low temperatures in the THz frequency range for all samples with $0.5 \leqslant x < 0.85$.

III. RESULTS AND ANALYSIS

Figure 1 presents the temperature evolution of the THz-infrared spectra of $\epsilon'(\nu)$ and $\sigma(\nu)$ of LCMO with a commensurate calcium content, $x = 2/3$. In the sub-phonon frequency range, below 100 cm^{-1}, unexpected modifications of the spectra occur in the CO state. Right below $T_{CO} = 240$ K, when the background conductivity of the free carriers freezes out, a bump becomes visible in $\sigma(\nu)$ at around 50 cm^{-1} [Fig. 1(b)]; at the lowest temperatures, at least two separate peaks can be distinguished. Below approximately 120 K an additional strong absorption band develops at slightly lower frequencies between 20 and 30 cm^{-1}; note, the intensity (spectral weight) in this spectral range grows significantly as the temperature decreases. In the linear presentation of $\sigma(\nu)$ [inset of Fig. 1(b)] the asymmetric line shape of the band becomes obvious; it is not possible to fit it by a Lorentzian. Related to this asymmetric band, the permittivity spectra exhibits an unusual dispersion [Fig. 1(a)] that becomes dominant when the temperature is reduced to 5 K. Note that the $\epsilon'(\nu)$ spectrum at $T = 5$ K exhibits an underdamped character of the absorption band, i.e., the permittivity first increases with frequency and then drops in the vicinity of the resonance frequency.

In Fig. 2 the development of the THz absorption bands is presented for the series of compounds with calcium contents $x = 0.5$, 0.6, 2/3, 0.7, 0.75, 0.85, 0.98. The commensurate composition $La_{0.25}Ca_{0.75}MnO_3$ was already discussed in Refs. 16, 17, and 18. It is important to note that in all samples that reveal a transition to the CO phase ($0.5 < x \leqslant 0.75$), the 50 cm^{-1} absorptions start to appear right below T_{CO}. For commensurate ($x = 2/3$) or almost commensurate ($x = 0.7$) calcium contents the strong lower-frequency resonance is clearly present. It always exhibits the pronounced asymmetric shape as discussed above [inset of Fig. 1(b)].

IV. DISCUSSION

Similar asymmetric absorption bands in LCMO were observed previously[8–12] and assigned to collective excitations

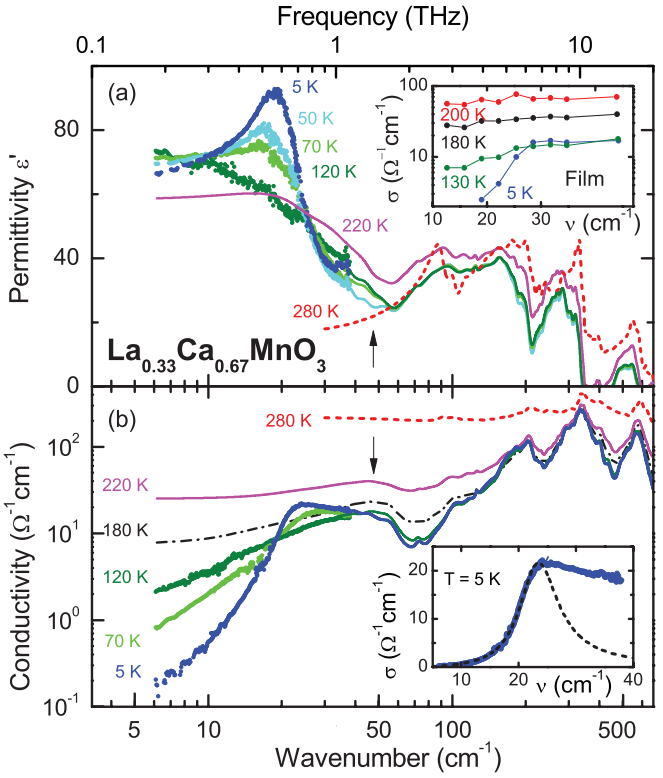

FIG. 1. (Color online) Temperature dependence of the optical properties of $La_{0.33}Ca_{0.67}MnO_3$ ceramic sample in the THz range. In the low-frequency part of (a) the dielectric permittivity $\epsilon'(\nu)$ and (b) the optical conductivity $\sigma(\nu)$, the charge order transition at $T_{CO} = 240$ K is seen as a dramatic change due to the opening of the energy gap in the far infrared. The arrows indicate the vibrational acoustic modes at 50 cm^{-1} that become infrared active by Brillouin zone folding due to charge ordering. The inset in panel (a) exhibits the temperature evolution of the THz conductivity measured on a thin epitaxial $La_{0.33}Ca_{0.67}MnO_3$ film. In the lower panel the inset demonstrates that it is not possible to fit the low-frequency asymmetrical band by a Lorentzian curve (dashed line).

of the CDW ground state. However, there are good arguments against this interpretation:[16,17] (i) The bands consist of two or even more spectral components that could only be explained by multiphonon Peierls coupling, as in the case of organic mixed stack compounds.[28] (ii) The pinned CDW modes are typically heavily overdamped,[29,30] in contrast to our observations [cf. the underdamped character of the dispersion of the permittivity spectra in Fig. 1(a) and in the inset in Fig. 2]. (iii) With increasing impurity concentration the pinning of the CDW condensate becomes firmer.[29] Thus one expects different frequencies of the pinned modes when varying the doping values x.[31] (iv) The dielectric contribution $\Delta\epsilon'$ of the CDW pinned modes can reach very high values (up to 10^4–10^6),[29] much larger than in the present case, where $\Delta\epsilon' \approx 30$–40 (inset of Fig. 2). (v) Unfortunately the determination of the activation energy is not very precise; nevertheless, the ratio $2\Delta/k_B T_{CO}$ estimated from the optical gap 2Δ appears rather large (approximately 6 to 30)[16,32] when compared to the mean-field value of 3.5.

We associate the observed low-energy absorption bands with acoustical lattice vibrations that become infrared

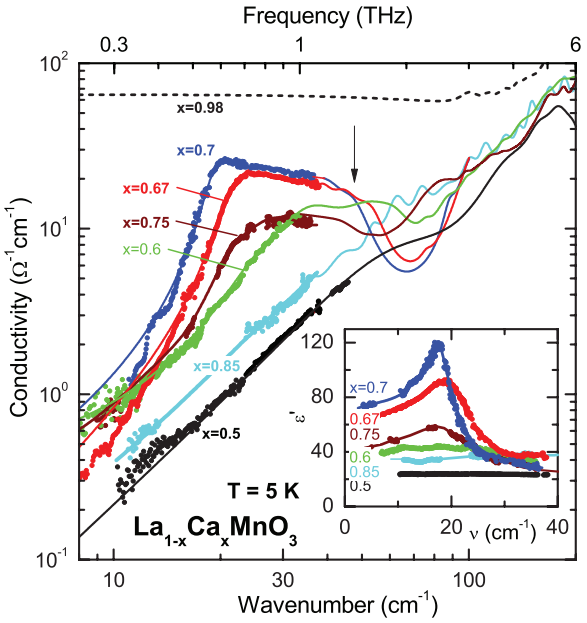

FIG. 2. (Color online) Development of the low-temperature terahertz conductivity of $La_{1-x}Ca_xMnO_3$ ceramics for different x. Close to $x = 2/3$ an asymmetric band develops around 20–30 cm^{-1}, that disappears again upon further doping. The charge-order activated folded modes are indicated by the arrow. Spectrum for $x = 0.75$ was taken on a pellet pressed of a powder.[16] The dielectric permittivity $\epsilon'(\nu)$ is displayed in the inset for the same compositions.

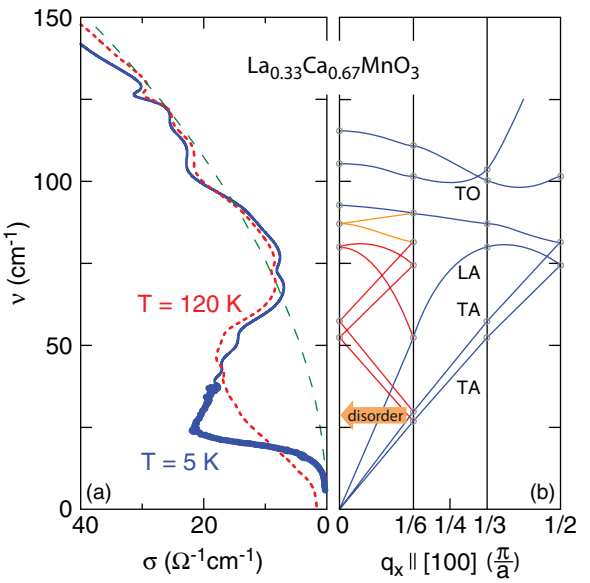

FIG. 3. (Color online) Explanation of the observed conductivity spectra (that is proportional to absorption) by the vibrational density of states. (a) Optical conductivity of $La_{0.33}Ca_{0.67}MnO_3$ at two different temperatures. The dashed line corresponds to a $\sigma(\nu) \propto \nu^2$ behavior. (b) Energy dispersion of lattice vibrations calculated for $CaMnO_3$. For commensurate doping $x = 2/3$ the Brillouin zone is folded to one third and the acoustic phonons become optical active around 50 cm^{-1}. In the case of disorder as in polycrystalline samples, a broad distribution with a maximum in the density of states around 25 cm^{-1} occurs, called the boson peak.

activated due to the Brillouin zone folding. The CO formation in manganites is accompanied by a lattice superstructure along the a direction with a period $a^* = a(1 - x)$; a is the lattice constant.[33,34] As demonstrated in Fig. 3(b) by a sketch of a Brillouin zone for the $x = 2/3$ compound, due to the triple folding of the Brillouin zone additional (folded) phonon modes should appear at around 50 cm^{-1}. In fact, they can be resolved in the spectra (arrow in Fig. 1) as weak peaks on the high-frequency shoulder of the pronounced 25 cm^{-1} band. This strong 25 cm^{-1}band, however, cannot be explained by a regular folded phonon, because it is located well below 50 cm^{-1}, where no folded phonons are expected, and most important, because it exhibits a remarkably asymmetric line shape. We argue that this asymmetric band represents the DOS of acoustical phonons that appears in the spectra due to the disordered nature of our polycrystalline samples.

The disorder-induced reconstruction of the low-energy part of the vibrational DOS $G(\nu)$ is known from glasses, amorphous materials, and similar disordered solids. It results in extra states, in addition to the Debye part that is proportional to the squared frequency ν^2, and is experimentally seen in the THz frequency range in the form of a peak in the reduced DOS $g(\nu) = G(\nu)/\nu^2$. This so-called boson peak[19,20] is one of the most discussed topics in disordered systems and marks some of the most puzzling open questions. Numerous models are formulated to explain the mechanisms of the boson peak (see Refs. 21 and 35–37 and references therein) but its origin is still not completely clear. Inelastic neutron scattering might be the best probe to observe the boson peak. Fortunately, due to the disorder-driven breakdown of the selection rules, it is also seen in optical spectra.[21–24] Based on numerical calculations[24] and experimental observations[37] the boson peak is associated with the critical points within the Brillouin zone, more specifically, with the lowest-energy van Hove singularity of the crystal. It commonly shows up at rather low frequencies when disorder is introduced.

The described signatures of the boson peak are in remarkable qualitative and even quantitative agreement with our data on $La_{1-x}Ca_xMnO_3$, where the polycrystalline nature of the samples should introduce a certain degree of disorder, such as the random distribution of the force constants and/or charge fluctuations at the grain boundaries. Indeed, the resonances in the spectra of LCMO samples with commensurate $x = 2/3$ and almost commensurate $x = 0.7$ concentrations emerge around 20–25 cm^{-1}, that is slightly below the lowest-energy van Hove singularities of the three-fold reduced Brillouin zone (cf. Figs. 1, 2, and 3), in full agreement with the theoretical prediction.[24] It should be pointed out that the asymmetric line shapes of these resonances closely resemble typical shapes of the vibrational DOS near the Brillouin zone critical points. It is interesting to compare the spectra of the ceramic sample with $x = 2/3$ to those of epitaxial films of the same composition, where the lower degree of disorder causes a significantly reduced strength of the boson peak, as can be seen in the inset of Fig. 1(a).

A boson peak in the phonon DOS may also become obvious in an additional term of the low-temperature lattice contribution to the heat capacity, e.g., by a deviation from Debye's T^3 power law. According to the general trend that noticeable contributions from a peak in the phonon DOS

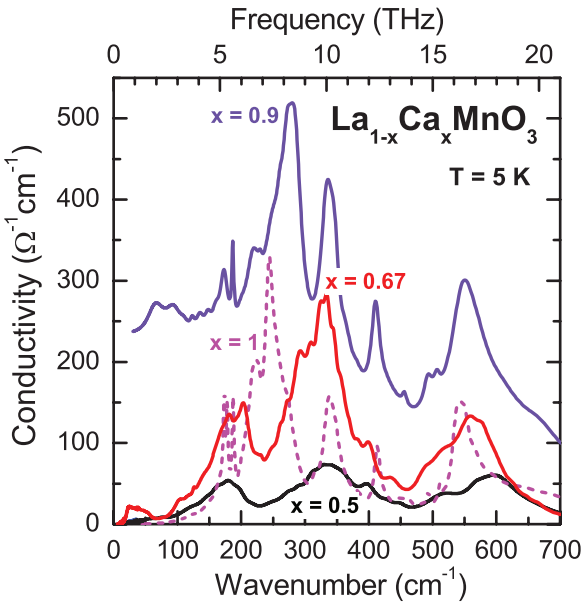

FIG. 4. (Color online) Phonon modes of $La_{1-x}Ca_xMnO_3$ for different $x = 0.5$, 2/3, 0.9, and 1. While for $x < 0.87$ three broad bands are observed that shift to lower frequencies as x increases, above $x = 0.87$ the absorption features change to a typical phonon spectrum.

become apparent at a temperature of $\sim 1/6$ of the peak energy,[38] we expect for $La_{0.33}Ca_{0.67}MnO_3$ deviations from the Debye law below 5 K. Our $C(T)$ measurements of $La_{0.33}Ca_{0.67}MnO_3$ down to 2 K indeed revealed additional low-temperature heat capacity contributions. At present, however, it is not clear whether additional magnetic terms have to be considered besides the extra contribution of the boson peak.

When turning to commensurate doping $x = 1/2$, we can understand from Fig. 3 that the phonon-related low-frequency features should be shifted to higher frequencies compared to the $x = 2/3$ compound, since the superlattice period is doubled (not tripled as for $x = 2/3$), i.e., the Brillouin zone should be reduced to $\pi/4a$ compared to $\pi/6a$. From Fig. 2 we see, however, that these features can hardly be resolved. The reason is that the composition $x = 1/2$ falls right on the boundary between the conducting ferromagnetic ($x < 0.5$) and insulating CO ($x > 0.5$) phases. The multiphase character of this compound masks the well-formed crystal lattice superstructure and blurs the Brillouin zone picture. In the case of the *incommensurate* value $x = 0.6$ the THz absorption band is quite pronounced and also asymmetric. This calcium content might be seen as a mixture of neighboring commensurate phases, $x = 1/2$ and 2/3;[15] accordingly the observed band is composed of folded phonons and of signatures of the boson peaks from these phases. For even higher doping level, $x = 0.85$, the THz spectra do not contain any structures because no CO develops and thus no superlattice exists. The same holds for the compound with $x = 0.98$ where, in addition, the high conductivity level screens out the THz structures.

In Fig. 4 the far-infrared spectra of some selected $La_{1-x}Ca_xMnO_3$ samples are presented on a linear scale in order to elucidate the phonons features. It is noticeable that the above-discussed acoustics-related excitations (folded phonons and boson peaks) are of significantly smaller amplitudes compared to the first-order phonon bands. This is an indication that charge order induces only a relatively small weight fraction of lattice modulations.[15] As for the first order phonon lines in $La_{1-x}Ca_xMnO_3$ that are presented in Fig. 4, the spectral density of phonon states for compounds with $0.5 \leqslant x < 0.87$ is composed by three continua that correspond to the transverse optical (TO) cubic perovskite modes TO1, TO2, and TO3. For commensurate modulations of the lattice (like for $x = 2/3$) the phonon resonances are well structured that is a consequence of transition to a long-periodic structure in the CO state. The phonon spectra change drastically when the concentrational phase-transition line is crossed at $x = 0.87$. The typical phonon response for higher concentrations (represented in Fig. 4 by the $x = 0.9$ spectrum) demonstrates a higher degree of order in the crystal lattice as compared to the $x < 0.87$ solid solutions. The phonon DOS for $CaMnO_3$ is typical for the rhombic perovskites of the *Pnma* symmetry with four molecules in the unit cell.

V. CONCLUSIONS

We have discovered several absorption bands in the terahertz spectra of overdoped manganites $La_{1-x}Ca_xMnO_3$ for commensurate calcium concentration below the charge-order transition T_{CO}. We identify acoustical phonon modes which are activated optically in the charge-ordered state, where the crystal lattice forms a superstructure and the corresponding Brillouin zone is folded back. Most important, we observe a pronounced extra absorption feature with strongly asymmetric line shape that we associate with the boson peak – a counterpart of the lowest-energy acoustic van Hove singularity at the boundary of the folded Brillouin zone that gains optical activity due to disorder. Our findings evidence that disorder effects must be taken into account when analyzing low-energy properties of overdoped manganites.

ACKNOWLEDGMENTS

We acknowledge financial suppoart by the Deutsche Forschungsgemeinschaft (DFG) via DR228/36, Russian State contracts N16.740.11.0467, 14.18.21.0740, RFBR project 11-02-91340-HHNO-a, and by the Natural Science Foundation of China Grant No. 10904146. We enjoyed discussions with S. N. Taraskin.

[1] A. P. Ramirez, J. Phys.: Condens. Matter **9**, 8171 (1997).
[2] E. Dagotto, *Nanoscale Phase Separation and Colossal Magnetoresistance* (Springer-Verlag, Berlin, 2003).
[3] M. B. Salamon and M. Jaime, Rev. Mod. Phys. **73**, 583 (2001).
[4] C. H. Chen and S.-W. Cheong, Phys. Rev. Lett. **76**, 4042 (1996); C. H. Chen, S.-W. Cheong, and H. Y. Hwang, J. Appl. Phys. **81**, 4326 (1997); S. Mori, C. H. Chen, and S.-W. Cheong, Nature (London) **392**, 473 (1998).

[5]G. C. Milward, M. J. Caldern, and P. B. Littlewood, Nature (London) **433**, 607 (2005).
[6]M. Tonouchi, Nat. Photon. **1**, 97105 (2007).
[7]Y.-G. Chuang, A. D. Gromko, D. S. Dessau, T. Kimura, and Y. Tokura, Science **292**, 1509 (2001).
[8]N. Kida and M. Tonouchi, Phys. Rev. B **66**, 024401 (2002).
[9]R. Rana, N. Awari, P. Pandey, A. Singh, S. S. Prabhu, and D. S. Rana, J. Phys.: Condens. Matter **25**, 106004 (2013).
[10]A. Nucara, P. Maselli, P. Calvani, R. Sopracase, M. Ortolani, G. Gruener, M. Cestelli Guidi, U. Schade, and J. Garcia, Phys. Rev. Lett. **101**, 066407 (2008); J. Supercond. Nov. Magn. **22**, 13 (2009).
[11]K. R. Mavani, M. Nagai, D. S. Rana, H. Yada, I. Kawayama, M. Tonouchi, and K. Tanaka, Appl. Phys. Lett. **93**, 231908 (2008).
[12]J. Fujioka, Y. Ida, Y. Takahashi, N. Kida, R. Shimano, and Y. Tokura, Phys. Rev. B **82**, 140409 (2010).
[13]R. Schmidt, Phys. Rev. B **77**, 205101 (2008).
[14]B. Fisher, J. Genossar, L. Patlagan, and G. M. Reisner, J. Magn. Magn. Mater. **322**, 1239 (2010).
[15]M. Pissas and G. Kallias, Phys. Rev. B **68**, 134414 (2003); M. Pissas, I. Margiolaki, K. Prassides, and E. Suard, *ibid.* **72**, 064426 (2005).
[16]T. Zhang, E. Zhukova, B. Gorshunov, D. Wu, A. S. Prokhorov, V. I. Torgashev, E. G. Maksimov, and M. Dressel, Phys. Rev. B **81**, 125132 (2010).
[17]E. Zhukova, B. Gorshunov, T. Zhang, Dan Wu, A. S. Prokhorov, V. I. Torgashev, E. G. Maksimov, and M. Dressel, Europhys. Lett. **90**, 17005 (2010).
[18]B. P. Gorshunov, E. S. Zhukova, E. G. Maksimov, A. S. Prokhorov, V. I. Torgashev, T. Zhang, D. Wu, and M. Dressel, JETP Lett. **91**, 336 (2010).
[19]*Amorphous Solids: Low Temperature Properties*, edited by W. A. Phillips (Springer, Berlin, 1981).
[20]S. R. Elliott, *Physics of Amorphous Materials*, 2nd edition (Longmans, New York, 1990).
[21]W. Schirmacher, G. Diezemann, and C. Ganter, Phys. Rev. Lett. **81**, 136 (1998).
[22]F. L. Galeener and P. N. Sen, Phys. Rev. B **17**, 1928 (1978); F. L. Galeener, A. J. Leadbetter, and M. W. Stringfellow, *ibid.* **27**, 1052 (1983).
[23]C. T. Kirk, Phys. Rev. B **38**, 1255 (1988).
[24]S. N. Taraskin, Y. L. Loh, G. Natarajan, and S. R. Elliott, Phys. Rev. Lett. **86**, 1255 (2001); S. N. Taraskin, S. I. Simdyankin, S. R. Elliott, J. R. Neilson, and T. Lo, *ibid.* **97**, 055504 (2006).
[25]V. Moshnyaga, I. Khoroshun, A. Sidorenko, P. Petrenko, A. Weidinger, M. Zeitler, B. Rauschenbach, R. Tidecks, and K. Samwer, Appl. Phys. Lett. **74**, 2842 (1999).
[26]G. Kozlov and A. Volkov, in *Millimeter and Submillimeter Wave Spectroscopy of Solids*, edited by G. Grüner (Springer, Berlin, 1998).
[27]B. P. Gorshunov, A. Volkov, I. E. Spektor, A. S. Prokhorov, A. A. Mukhin, M. Dressel, S. Uchida, and A. Loidl, Int. J. Infrared Millimeter Waves **26**, 1217 (2005).
[28]A. Girlando, M. Masino, A. Painelli, N. Drichko, M. Dressel, A. Brillante, R. G. Della Valle, and E. Venuti, Phys. Rev. B **78**, 045103 (2008).
[29]G. Grüner, *Density Waves in Solids* (Addison-Wesley, Reading, 1994).
[30]S. Cox, J. Singleton, R. D. McDonald, A. Migliori, and P. B. Littlewood, Nature (London) **7**, 25 (2008).
[31]L. Degiorgi, B. Alavi, G. Mihály, and G. Grüner, Phys. Rev. B **44**, 7808 (1991).
[32]K. H. Kim, S. Lee, T. W. Noh, and S.-W. Cheong, Phys. Rev. Lett. **88**, 167204 (2002).
[33]S. Larochelle, A. Mehta, N. Kaneko, P. K. Mang, A. F. Panchula, L. Zhou, J. Arthur, and M. Greven, Phys. Rev. Lett. **87**, 095502 (2001).
[34]J. C. Loudon, S. Cox, A. J. Williams, J. P. Attfield, P. B. Littlewood, P. A. Midgley, and N. D. Mathur, Phys. Rev. Lett. **94**, 097202 (2005); S. Cox, E. Rosten, J. C. Chapman, S. Kos, M. J. Calderon, D. J. Kang, P. B. Littlewood, P. A. Midgley, and N. D. Mathur, Phys. Rev. B **73**, 132401 (2006).
[35]S. N. Taraskin and S. R. Elliott, Phys. Rev. B **59**, 8572 (1999).
[36]V. L. Gurevich, D. A. Parshin, and H. R. Schober, Phys. Rev. B **67**, 094203 (2003).
[37]A. I. Chumakov, G. Monaco, A. Monaco, W. A. Crichton, A. Bosak, R. Rüffer, A. Meyer, F. Kargl, L. Comez, D. Fioretto, H. Giefers, S. Roitsch, G. Wortmann, M. H. Manghnani, A. Hushur, Q. Williams, J. Balogh, K. Parlin'ski, P. Jochym, and P. Piekarz, Phys. Rev. Lett. **106**, 225501 (2011).
[38]M. Cardona, R. K. Kremer, G. Siegle, A. Munoz, A. H. Romero, and M. Schmidt, Phys. Rev. B **82**, 085210 (2010).